Communication

Low-Temperature Solution Synthesis of the Non-Equilibrium Ordered Intermetallic Compounds AuFe, AuCo, and AuNi as Nanocrystals

Yolanda Vasquez, Zhiping Luo, and Raymond E. Schaak

J. Am. Chem. Soc., **2008**, 130 (36), 11866-11867 • DOI: 10.1021/ja804858u • Publication Date (Web): 16 August 2008

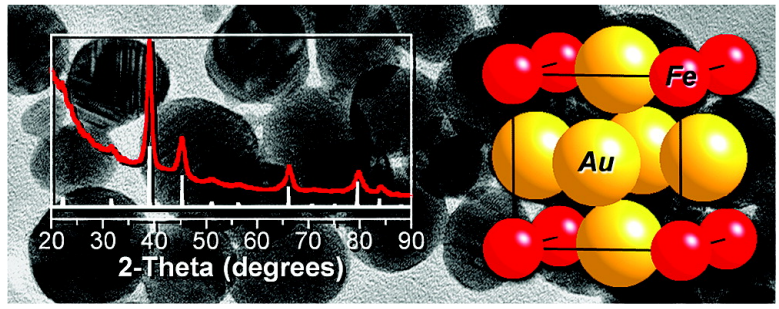

More About This Article

Additional resources and features associated with this article are available within the HTML version:

- Supporting Information
- Access to high resolution figures
- Links to articles and content related to this article
- Copyright permission to reproduce figures and/or text from this article

View the Full Text HTML

J|A|C|S
COMMUNICATIONS

Published on Web 08/16/2008

Low-Temperature Solution Synthesis of the Non-Equilibrium Ordered Intermetallic Compounds Au_3Fe, Au_3Co, and Au_3Ni as Nanocrystals

Yolanda Vasquez,[†] Zhiping Luo,[‡] and Raymond E. Schaak*[,†,§]

Department of Chemistry and Microscopy and Imaging Center, Texas A&M University, College Station, Texas 77843, and Department of Chemistry and Materials Research Institute, The Pennsylvania State University, University Park, Pennsylvania 16802

Received June 25, 2008; E-mail: schaak@chem.psu.edu

Alloys and intermetallic compounds of Au with the magnetic 3d elements Fe, Co, and Ni are fascinating materials because they are nonequilibrium phases that are of interest for their catalytic, magnetic, optic, and magneto-optic properties.[1−3] For example, Au−Fe alloys exhibit spin glass behavior and chiral susceptibility,[2] as well as combined plasmonic and superparamagnetic properties as nanoparticles.[3] Despite the immiscibility gap that exists between Au and the magnetic 3d elements, several methods have succeeded at preparing a variety of atomically disordered Au−M (M = Fe, Co, Ni) alloys.[1−3] However, the atomically ordered nonequilibrium Au−M intermetallics are often the subject of theoretical prediction[4] but, for the most part, remain elusive experimentally. $L1_0$-type AuFe has been artificially fabricated by depositing and annealing alternating monolayers of Au and Fe,[5] as well as by vacuum annealing of Au nanoparticles overgrown with Fe via evaporation.[6] Au−Ni and Au−Co intermetallics have occasionally been observed via interfacial diffusion, coevaporation, and ion beam manipulation.[7] To the best of our knowledge, there have been no reports of $L1_2$-type Au_3M intermetallics formed as isolatable solids. Here we report the synthesis of the ordered intermetallic compounds Au_3Fe, Au_3Co, and Au_3Ni with the $L1_2$ (Cu_3Au) structure as nanocrystals using low-temperature solution chemistry techniques.

The synthesis was modified from a procedure published by Zhou et al.[8] In a typical reaction, $HAuCl_4 \cdot 3H_2O$ (10.0 mg), oleylamine (50 μL), and the appropriate amount of $Fe(acac)_3$, $Co(acac)_2$, or $Ni(acac)_2$ to yield a 3:1 molar ratio were added to 5 mL of octyl ether and heated to 80 °C under Ar. Then, 0.7 mL of 2.81 M *n*-butyllithium was added quickly via syringe to 10 mL of octyl ether, also at 80 °C and under Ar. Finally, the 5-mL octyl ether metal salt solution at 80 °C was added quickly via syringe. The reaction mixture was heated to 250 °C, the heat was turned off, and the sample was cooled to room temperature. The product was isolated by adding 10 mL of ethanol, centrifuging at 13 krpm, then extracting into the toluene layer of a toluene/water mixture.

Figure 1 shows the powder XRD pattern for Au_3Fe, which matches that expected for the cubic $L1_2$ structure. The lattice constant (a = 3.99 Å) is contracted relative to that of pure Au (a_{Au} = 4.07 Å), and the *100*, *110*, *210*, *211*, and *221* superlattice peaks characteristic of the $L1_2$ structure are clearly evident. Figure 2 shows the powder XRD data for Au_3Co (a = 4.00 Å) and Au_3Ni (a = 4.00 Å), which also have the expected $L1_2$ superlattice peaks.

The Au−Co system provides insight into the reaction pathway that results in the formation of the nonequilibrium intermetallics. The original idea was that the rapid coreduction of the metal reagents afforded by the strong reducing agent would allow them to effectively conucleate.[8] Figure 2b shows XRD data for aliquots

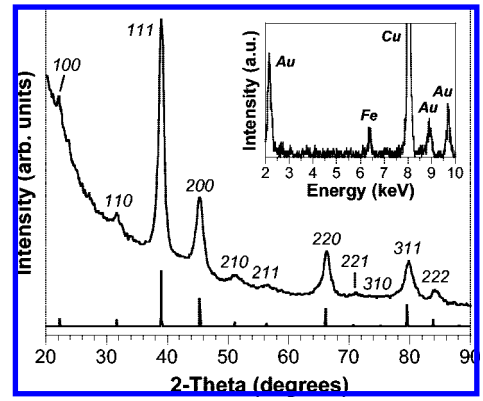

Figure 1. Experimental (top) and simulated (bottom) powder XRD patterns for $L1_2$-type Au_3Fe. (Inset) EDS spectrum for Au_3Fe nanocrystals.

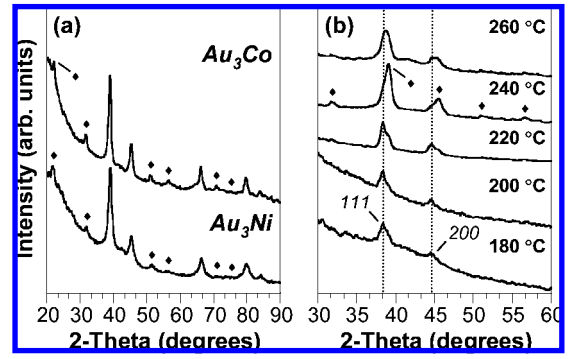

Figure 2. (a) Powder XRD data for Au_3Co and Au_3Ni. Diamonds (◆) indicate the $L1_2$ superlattice peaks. (b) Powder XRD data for aliquots taken during the synthesis of Au_3Co. Vertical lines correspond to the *111* and *200* peak positions for Au, and the diamonds (◆) denote the peaks corresponding to $L1_2$-type Au_3Co.

taken during the formation of Au_3Co nanocrystals. At 180 °C, the crystalline product matches well with pure Au. Au is also the predominant product at 200 °C, with Au_3Co beginning to appear by 220 °C. By 240 °C, the predominant product is Au_3Co. This shows that Au nucleates first, and the 3*d* transition metal reacts with the Au nanoparticles to form the Au_3M intermetallics. This is analogous to stepwise reaction pathways we have observed in the formation of other binary and ternary intermetallics using low-temperature solution routes.[9] Interestingly, continued heating beyond 260 °C causes the superlattice peaks to disappear. This implies that the disordered alloy is the favored product and the ordered intermetallic is kinetically stabilized by low temperatures and short heating times. It is worth noting that attempts to form the Au_3M intermetallics using other common solution reduction

[†] Department of Chemistry, Texas A&M University.
[‡] Microscopy and Imaging Center, Texas A&M University.
[§] The Pennsylvania State University.

10.1021/ja804858u CCC: $40.75

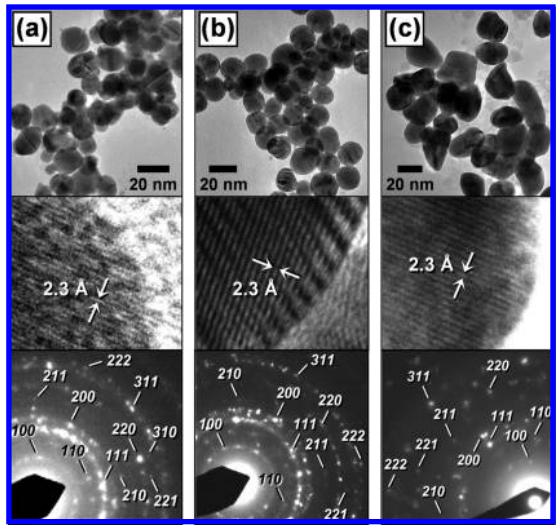

Figure 3. TEM images (top), high-resolution TEM images showing *111* lattice fringes (middle), and electron diffraction patterns (bottom) for $L1_2$-type (a) Au_3Fe, (b) Au_3Ni, and (c) Au_3Co nanocrystals.

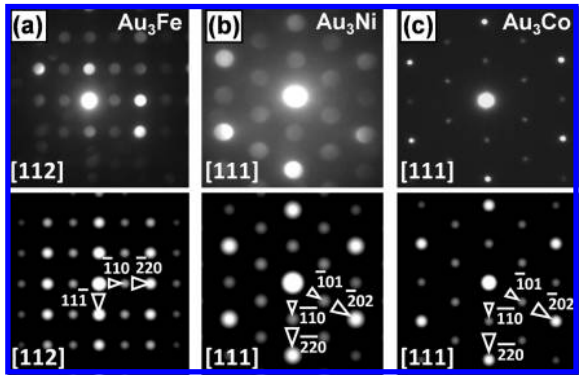

Figure 4. Nanobeam electron diffraction (NBED) patterns for individual nanocrystals of (a) Au_3Fe along the [112] zone axis and (b) Au_3Ni along the [111] zone axis. Selected-area electron diffraction pattern for a single Au_3Co nanocrystal along the [111] zone axis is shown in (c). (Top) experimental; (bottom) simulated.

techniques were unsuccessful in our hands, demonstrating that the reduction kinetics still play an important role in the reaction.

Figure 3 shows TEM micrographs and selected area electron diffraction (SAED) patterns for the Au_3M nanocrystals. The Au_3Fe and Au_3Ni nanocrystals are generally spherical with an average particle size of around 20 nm, ranging from 15−30 nm throughout the sample. The Au_3Co nanocrystals are slightly larger with more elongation and faceting. High-resolution TEM micrographs of individual particles (Figures 3 and S1, Supporting Information) show that the nanocrystals are highly crystalline with lattice fringes of 2.3 Å, corresponding to the *111* plane of the Au_3M intermetallics. The SAED patterns shown in Figure 3 also confirm the formation of the $L1_2$-type intermetallics, with the *100*, *110*, *210*, *211*, and *221* superlattice reflections clearly evident. The EDS data for Au_3Fe (Figure 1) indicate a 3:1 ratio of Au:Fe, and EDS data confirm the stoichiometry of Au_3Co and Au_3Ni as well. All of the data are consistent with a bulk sample of Au_3M nanocrystals that crystallize in the ordered $L1_2$-type intermetallic structure.

Nanobeam electron diffraction (NBED) patterns provide additional evidence for the formation of the Au_3M intermetallics. The NBED patterns were taken using a beam size of 10 nm in diameter on single isolated nanoparticles that were confirmed by EDS to have a stoichiometry of Au_3M. Figure 4a and b show the NBED patterns from single Au_3Fe and Au_3Ni nanocrystals along the [112] and [111] zone axes, respectively. The strong reflection spots are from the fundamental fcc lattice (larger arrowheads, space group $Fm\bar{3}m$)[1] whereas the weak superlattice reflections (smaller arrowheads) appear at the half-positions of the fundamental reflections. This implies a primitive structure, consistent with the $L1_2$ superstructure (space group $Pm\bar{3}m$). Simulations using $L1_2$-type Au_3Fe and Au_3Ni as a model (Figure 4a and b) are consistent with the experimental patterns and further support the formation of $L1_2$-type nanocrystals. The slightly asymmetric intensity distribution of the NBED patterns is due to a small specimen tilt, and some extra spots are from surrounding particles. Figure 4c shows a SAED pattern collected along the [111] zone axis of a single Au_3Co nanocrystal (Figure S1, Supporting Information). This pattern, which is indicative of a single-domain particle, shows a strong contrast between the fundamental fcc lattice reflections and the superlattice reflections at the half-positions. The experimental data are consistent with the simulated data, providing additional evidence for the proposed $L1_2$ structure.

The Au_3M nanocrystal samples have small amounts of Au and MO_x impurities that complicate property measurements, and we cannot rule out the possibility that small amounts of impurities help to stabilize the $L1_2$ structure. We also cannot discount the possibility that the $L1_2$ intermetallics are stable low-temperature phases that have been inaccessible using traditional high-temperature methods. However, the formation of the Au_3M ordered intermetallics is still a significant result, since these phases have been elusive, yet of interest for their magnetic, optical, and catalytic properties. Further optimization should yield samples appropriate for property measurements, and similar methods could yield other nonequilibrium intermetallics.

Acknowledgment. This work was supported by the U.S. Department of Energy (DE-FG02-06ER46333), a Beckman Young Investigator Award, a Sloan Research Fellowship, a DuPont Young Professor Grant, and a Camille Dreyfus Teacher-Scholar Award. TEM was performed at the Texas A&M Microscopy and Imaging Center.

Supporting Information Available: Experimental details and additional TEM and NBED data. This material is available free of charge via the Internet at http: //pubs.acs.org.

References

(1) (a) Lahr, D. L.; Ceyer, S. T. *J. Am. Chem. Soc.* **2006**, *128*, 1800–1801. (b) Auten, B. J.; Hahn, B. P.; Vijayaraghavan, G.; Stevenson, K. J.; Chandler, B. D. *J. Phys. Chem. C* **2008**, *112*, 5365–5372. (c) Mader, S.; Nowick, A. S. *Appl. Phys. Lett.* **1965**, *7*, 57–59. (d) Lee, Y. P.; Kudryavtsev, Y. V.; Nemoshkalenko, V. V.; Gontarz, R.; Rhee, J. Y. *Phys. Rev. B* **2003**, *67*, 104424–8. (e) Canet, F.; Bellouard, C.; Joly, L.; Mangin, S. *Phys. Rev. B* **2004**, *69*, 094402.
(2) (a) Taniyama, T.; Ogawa, R.; Sato, T.; Ohta, E. *Mater. Sci. Eng., A* **1996**, *217*−*218*, 319–321. (b) Taniguchi, T.; Yamanaka, K.; Sumioka, H.; Yamazaki, T.; Tabata, Y.; Kawarazaki, S. *Phys. Rev. Lett.* **2004**, *93*, 246605–4.
(3) Chiang, I-C.; Chen, D.-H. *Adv. Funct. Mater.* **2007**, *17*, 1311–1316.
(4) (a) Sargolzaei, M.; Opahle, I.; Richter, M. *Phys. Status Solidi B* **2006**, *243*, 286–289. (b) Kong, Y.; Kong, L. T.; Liu, B. X. *J. Phys.: Condens. Matter* **2006**, *18*, 4345–4353. (c) Reichert, H.; Schops, A.; Ramsteiner, I. B.; Bugaev, V. N.; Shchyglo, O.; Udiansky, A.; Dosch, H.; Asta, M.; Drautz, R.; Honkimaki, V. *Phys. Rev. Lett.* **2005**, *95*, 235703. (d) Wolverton, C.; Zunger, A. *Comput. Mater. Sci.* **1997**, *8*, 107–121.
(5) Takanashi, K.; Mitani, S.; Sano, M.; Fujimori, H.; Nakajima, H.; Osawa, A. *Appl. Phys. Lett.* **1995**, *67*, 1016–1018.
(6) Sato, K.; Bian, B.; Hirotsu, Y. *Jpn. J. Appl. Phys.* **2002**, *41*, L1–3.
(7) (a) Kao, T.-H.; Song, J.-M.; Chen, I.-G.; Dong, T.-Y.; Hwang, W.-S. *Nanotechnology* **2007**, *18*, 435708. (b) Yan, H. F.; Guo, H. B.; Shen, Y. X.; Li, J. H.; Liu, B. X. *Acta Mater.* **2006**, *54*, 5293–5304. (c) Nabika, H.; Akamatsu, K.; Mizuhata, M.; Kajinami, A.; Deki, S. *J. Mater. Chem.* **2002**, *12*, 2408–2411. (d) He, J. H.; Carosella, C. A.; Hubler, G. K.; Qadri, S. B.; Sprague, J. A. *Phys. Rev. Lett.* **2006**, *96*, 056105–4.
(8) Zhou, S.; Jackson, G. S.; Eichhorn, B. *Adv. Funct. Mater.* **2007**, *17*, 3099–3104.
(9) (a) Leonard, B. M.; Schaak, R. E. *J. Am. Chem. Soc.* **2006**, *128*, 11475–11482. (b) Cable, R. E.; Schaak, R. E. *Chem. Mater.* **2007**, *19*, 4098–4104.

JA804858U